Draft version June 1, 2026
Typeset using LaTeX **twocolumn** style in AASTeX7.0.1

Super-Eddington accretion of black holes in early nuclear bursts gives birth to Little Red Dots

Yangyao Chen [1,2] and Houjun Mo [3]

[1] School of Astronomy and Space Science, Nanjing University, Nanjing, Jiangsu 210093, China
[2] Key Laboratory of Modern Astronomy and Astrophysics, Nanjing University, Ministry of Education, Nanjing, Jiangsu 210093, China
[3] Department of Astronomy, University of Massachusetts, Amherst, MA 01003, USA

ABSTRACT

In a recent paper, Chen et al. developed a framework for modeling the seeding and growth of supermassive black holes (BHs) in the context of ΛCDM cosmogony. Here, we use a set of physically motivated criteria to select a population of predicted BHs and link them to Little Red Dots (LRDs) discovered by JWST. We show that the LRD population at high redshift (z) emerges naturally from a subset of BHs with super-Eddington accretion during nuclear bursts. The model suggests that the observed LRDs are the "tip of the iceberg" of a much larger population of less luminous BHs in the same subset. The model makes specific predictions for the LRD population, such as the mass distributions of their BHs and host galaxies/halos, and the piece-wise redshift evolution of their number density. The cosmological context of the model also allows us to link the observed LRD population to their progenitors (their BH seeds) and lower-z descendant BHs, galaxies and halos. Most LRDs at $z \sim 5$ are seeded at $z \gtrsim 20$ through direct-collapse BHs or pair-instability supernovae from Pop-III stars, and have grown to $M_{\rm BH} \approx 10^5$–$10^7\,{\rm M}_\odot$ through nuclear bursts by their observed redshift. LRDs are predicted to have diverse descendants, ranging from compact dwarf galaxies to brightest cluster galaxies (BCGs) at $z = 0$. These predictions are consistent with current observations and can be further tested. The success of this model indicates that the results presented here provide a robust foundation for building detailed models of the LRD population.

Keywords: Galaxy formation (595) — Active galactic nuclei (16) — AGN host galaxies (2017) — Supermassive black holes (1663)

1. INTRODUCTION

Recent JWST observations unveiled a population of Little Red Dots (LRDs) at high redshift (z), characterized by compact morphology, a peculiar V-shape spectral energy distribution (SED), the presence of broad emission lines, and a number density much higher than that of known quasars (e.g. J. Matthee et al. 2024; V. Kokorev et al. 2024; J. E. Greene et al. 2024; P. G. Pérez-González et al. 2024; H. B. Akins et al. 2025; I. Labbe et al. 2025; C.-H. Chen et al. 2025; Z. Li et al. 2025). Follow-up multi-wavelength observations showed that LRDs are deficient in X-ray, infrared, submillimeter and radio emission (M. Yue et al. 2024; K. Perger et al. 2025; H. B. Akins et al. 2025; J. E. Greene et al. 2026). These observed properties of LRDs are distinct from known populations of active galactic nuclei (AGNs) and galaxies, making their existence an interesting problem for galaxy formation and black hole (BH) growth in the ΛCDM cosmogony.

Much effort has been put into understanding the nature and origin of LRDs. Hypotheses that have been proposed and examined include changing the properties of dust to accommodate the peculiar shape of the observed SED (Z. Li et al. 2025); invoking scattered light from the AGN and young stellar population to explain the rest-frame UV part of the SED (J. E. Greene et al. 2024; I. Labbe et al. 2025; K. Inayoshi et al. 2026); associating the central BH with a stellar-like envelope (A. de Graaff et al. 2025; D. Kido et al. 2025; R. P. Naidu et al. 2025a; K. Inayoshi et al. 2026); linking LRDs to the formation of BH seeds (M. C. Begelman & J. Dexter 2026; J. F. W. Baggen et al. 2026) to produce the rest-frame red part of the SED; assuming the gas column density to be in the Compton-thick regime to produce the lack of X-ray emission (H. Liu et al. 2025; X. Ji et al. 2025a; R. P. Naidu et al. 2025a); and assuming self-interacting dark matter to transport heat outward so as to produce collapsed central objects in dark matter halos (F. Jiang et al. 2025; Z. Wang et al. 2026; M. G. Roberts et al. 2026). These efforts provide important insights into the parameter space that could be relevant to the formation of LRDs. However, a self-consistent and coherent scenario in the context of the current structure-formation paradigm is still lacking.

Email: yangyaochen.astro@foxmail.com, hjmo@umass.edu

The main challenge in modeling the formation of LRDs from first principles comes from the complex interplay among processes operating in the high-z universe and the large dynamic ranges involved. For example, the interpretation based on ongoing seeding events invokes strong heating to suppress the fragmentation of gas and star formation prior to the observed epochs of LRDs (e.g. J. F. W. Baggen et al. 2026; see also T. H. Greif et al. 2011; J. H. Wise et al. 2019; M. A. Latif et al. 2022 for alternative heating mechanisms). However, at $z \approx 5$ when LRDs are abundant, previous star formation may already have enriched the intergalactic medium (IGM; e.g. Fig. D4 of Paper-IV; D. Spinoso et al. 2023), which makes the effectiveness of such heating questionable. The solution with a gas envelope and nuclear star formation surrounding the BH may be able to reproduce the observed SED (e.g. A. de Graaff et al. 2025; D. Kido et al. 2025; R. P. Naidu et al. 2025a; K. Inayoshi et al. 2026), but complex baryon cycles, associated with the expected bursty star formation for small galaxies at high z (K. El-Badry et al. 2016; J. Stern et al. 2021; P. F. Hopkins et al. 2023; Y. Asada et al. 2024; Q. Ma et al. 2026), make the depletion and replenishment of gas highly uncertain. Modeling these processes using current cosmological hydrodynamical simulations suffers from uncertainties in sub-grid implementation, such as artificial seeding of BHs and simplified treatment of BH accretion and feedback (e.g. D. Sijacki et al. 2007; R. Weinberger et al. 2017; S. Koudmani et al. 2024; H. Li et al. 2025). Idealized and zoom-in simulations (e.g. K.-Y. Su et al. 2023; P. F. Hopkins et al. 2024; A. Sivasankaran et al. 2025) may miss the cosmological context and lack the power to make statistical predictions.

Recently, Y. Chen et al. (2025a, hereafter Paper-IV) constructed a physical framework to seed and grow BHs together with their host galaxies and halos within the ΛCDM cosmogony. This model is based on the two-phase scenario of galaxy formation proposed by H. Mo et al. (2024, hereafter Paper-I), with key extensions needed to account for the seeding and early growth of BHs. The model tackles the aforementioned challenge by self-consistently modeling the complex interplay among processes relevant to BH seeding and growth, and uses semi-analytical approximations with multi-layer numerical refinements to achieve the resolution needed to cover the full structure hierarchy from large-scale structures to the surroundings of BHs. As shown in Y. Chen et al. (2024, hereafter Paper-II), Y. Chen et al. (2025b, hereafter Paper-III) and Paper-IV, the model not only reproduces a wide range of observed properties of BHs and their host galaxies/halos, but also predicts the evolution histories of BHs from their seeding times to $z = 0$. It is therefore interesting to study whether the model can yield a population of objects that resemble the observed LRDs. In particular, the cosmological context of the model allows us to investigate not only the physical mechanisms that give birth to LRDs but also their fates and links to other objects at lower-z. As we show, our model predicts a branch of BHs that are in super-Eddington accretion during nuclear bursts. A subset of these BHs closely resemble the observed LRDs in accretion rates and in BH mass to stellar mass ratios, and the model can be used to predict their number density, their host galaxy/halo and descendant properties.

This paper is organized as follows. In §2, we summarize the model of galaxy formation and BH growth, and we define the selection criteria for LRDs. In §3, we present model predictions for LRDs, their host galaxies/halos, and their descendants. In §4, we summarize our results and discuss their implications.

2. THE METHOD

Here we first provide a brief description of the model of galaxy formation and BH growth developed in Paper-IV. We then define criteria to select LRDs from the predicted properties of BHs and host galaxies.

2.1. *The model of galaxy formation and black hole growth*

The model takes halo merger trees from TNG100-1-Dark (A. Pillepich et al. 2018; D. Nelson et al. 2019). The simulation, the same as used in Paper-IV, has a periodic box of $75\,h^{-1}$Mpc on a side and a particle mass of $6.0 \times 10^6\,h^{-1}\mathrm{M}_\odot$. The cosmology adopted in the simulation is a flat ΛCDM cosmology (Planck Collaboration et al. 2016), with parameters of $h = 0.6774$, $\Omega_{\rm m,0} = 0.3089$, $\Omega_{\Lambda,0} = 0.6911$, $\Omega_{\rm b,0} = 0.0486$, and a Gaussian initial power spectrum specified by $n_{\rm s} = 0.9667$ and $\sigma_8 = 0.8159$. The same cosmology is assumed in our analysis.

The sample of simulated subhalos used here is selected to have $M_{\rm halo} \geq 10^{9.5}\,\mathrm{M}_\odot$ at $z = 0$ for a central subhalo and at the time of infall for a satellite subhalo. The assembly history of each subhalo is constructed directly from the simulation above a mass limit of $5 \times 10^8\,h^{-1}\mathrm{M}_\odot$. An extension algorithm is applied to trace the assembly history of each halo further back to a mass of $M_{\rm halo} \approx 10^5\,\mathrm{M}_\odot$ (see Appendix D1 of Paper-IV), so that processes leading to the formation of the first-generation stars and BH seeds in the halo can be modeled. This eliminates the need for artificially assigning massive BH seeds to halos (e.g. R. S. Somerville et al. 2008; R. A. Crain et al. 2015; R. Weinberger et al. 2017), which is crucial as LRDs may be powered by BHs of relatively low mass. The use of simulated halos also allows us to model the environments of individual halos.

A seeding procedure is applied to each assembly history to identify the epoch of first collapse of the halo gas and to determine the properties of first-generation stars and BH seeds formed in the collapsed gas (see §2.3 of Paper-IV). The key components of the seeding procedure can be summarized as follows.

1. An environmentally modulated criterion for gas collapse. Here internal coolants (H and H_2) are evaluated to identify the halo mass $M_{\rm halo}$ at which gas in a pristine halo

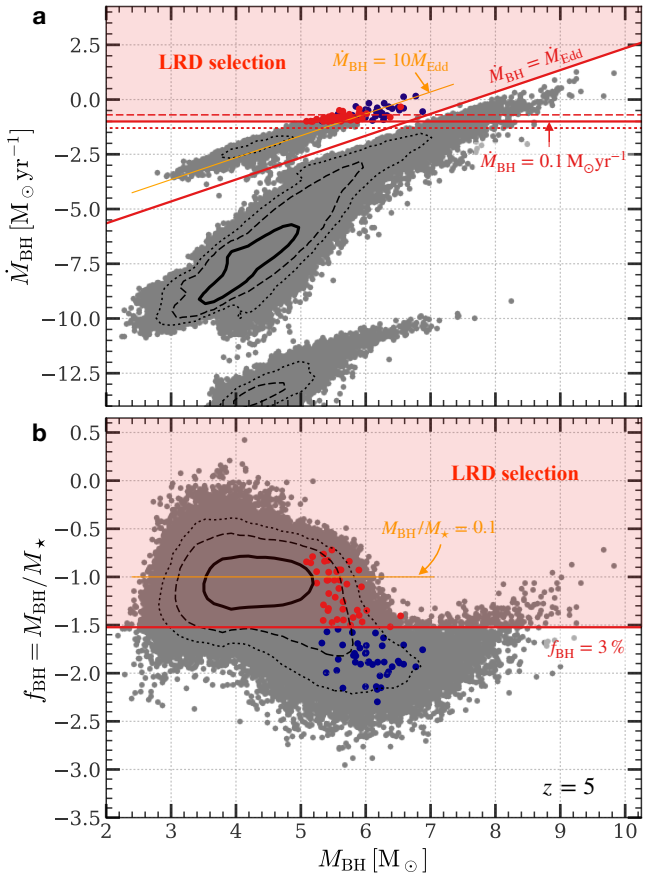

Figure 1. Selection of LRDs. Each dot represents a BH produced by the model at $z = 5$ in the planes of **a**, BHAR ($\dot{M}_{\rm BH}$) versus BH mass, and **b**, BH-mass fraction ($f_{\rm BH} \equiv M_{\rm BH}/M_\star$) versus BH mass. In each panel, **contours** from inner to outer encompass 68%, 95% and 99.7%, respectively, of all BHs. **Orange line** indicates the typical $\dot{M}_{\rm BH}$ or $f_{\rm BH}$ of the bursty branch. The default selection criterion for LRDs is marked by **red shading** enclosed by **red solid lines**, and LRDs so selected are shown by **red dots**. BHs passing the selection for $\dot{M}_{\rm BH}$ but not for $f_{\rm BH}$ are shown by **blue dots**. **Red dashed and dotted lines** in **a** show alternative selection criteria with varied thresholds of BHAR. The figure shows that the observed LRDs are the tip of the branch shaped by nuclear bursts (see §2.2 for details).

can effectively cool and collapse. Three environmental effects that can advance or delay the collapse are included: the Lyman-Werner (LW) radiation produced by other galaxies, which can dissociate H_2 and thus delay the collapse; the dynamical heating due to fast halo accretion in the early Universe, which can heat the halo gas and thus also delay the collapse; the enrichment of the IGM, which can feed coolants into the halo and thus can advance the collapse.

2. A feedback-regulated initial mass function (IMF). Here, the feedback from the first Pop-III star cluster formed in the collapsed gas of a pristine halo is evaluated to determine the resulting mass of individual stars in the cluster.
3. A 'multi-flavor' stellar evolution. Here, the evolution of individual stars in the first cluster is followed according to their initial masses. The mass of the most massive star in the cluster determines whether a core-collapse supernova (CCSN), a pair-instability supernova (PISN), or a direct collapse black hole (DCBH) can occur. The most massive BH remnant in the cluster is then defined as the seed of the central BH, while other stars constitute the initial stellar component of the host galaxy.

Thus, for each halo, the output of the seeding procedure is the initial $M_\star$ of the galaxy, the $M_{\rm BH}$ of the BH seed, as well as the flavor (DCBH, PISN or CCSN) that represents the evolution pathway of the most massive star in the first star cluster.

A growing procedure then starts with the initial conditions set by the seeding procedure to model the post-seeding growth of the BHs and their host galaxies (see §2.4 of Paper-IV). The key feature here is the multi-channel growth of BHs, with each channel representing a way to generate dynamical hotness, to remove the angular-momentum barrier, and to feed baryons to the central BH. These channels can be summarized as follows.

1. The bursty mode, which appears as rapid BH growth via super-Eddington accretion associated with intense starbursts in the dense gaseous nucleus formed under a global disturbance of the host galaxy. The gas density of such a nucleus can reach a 'supernova-free' threshold, $n_{\rm snf} \equiv 10^{3.5}\,{\rm cm}^{-3}$, corresponding to a dynamical timescale of $t_{\rm dyn,snf} = 0.75\,{\rm Myr}$ that is too short for the feedback of massive stars to be important. The consequence of the formation of such a nucleus is a "nuclear burst" characterized by super-Eddington accretion of the central BH, intense star formation that grows the nuclear star cluster (NSC), and strong BH feedback that disperses the nucleus. The trigger of a nuclear burst is modeled once the host halo temporarily experiences an excursion of fast assembly that brings in a large amount of matter so as to disturb the gravitational potential of the host galaxy significantly. The duration of a nuclear burst is $\lesssim t_{\rm dyn,snf}$ before the mode is quenched and another excursion is triggered.
2. The continuous mode, in which the BH continuously captures sub-clouds seeded and amplified by the turbulence in the self-gravitating gas cloud (SGC; see Paper-I for the concept) formed during the fast assembly phase of a halo. The associated star formation in the SGC is to build an extended, dynamically hot stellar component (bulge) of the host galaxy. In contrast, the collapse of the gas in the slow phase of a halo is expected to form a dynamically cold disk in which the growth of the BH ceases.
3. The merger mode, in which two galaxies and their central BHs merge to form a new galaxy and a new central BH.

These channels are not mutually exclusive at a given time during the post-seeding growth of a BH. However, the dominating channel transits sequentially from the bursty mode, via the continuous mode, to the merger mode over the lifetime of a BH (see §3.2 of Paper-IV). As will be shown in §3.1, the transition of the dominant channel is the key to explaining the observed evolution in the number density of LRDs over cosmic time. The product of the growing procedure is the properties of BHs and their host galaxies/halos, as well as the contribution of each growth channel to the total growth, from the seeding epoch to $z = 0$.

Since the duration of a nuclear burst is much shorter than the simulation snapshot interval, we assume that it occurs over a random duration $[t, t + t_{\rm dyn,snf}]$, where t is sampled uniformly from the time interval spanned by the snapshot in which the trigger is identified. The black hole accretion rate (BHAR, denoted as $\dot{M}_{\rm BH}$) during the burst is then calculated as the ratio between $\Delta M_{\rm BH}$ and $t_{\rm dyn,snf}$.

Fig. 1a shows the distribution of individual BHs predicted by the model at $z = 5$ in the $\dot{M}_{\rm BH}$-$M_{\rm BH}$ plane. A prominent multi-modal distribution can be seen. The dominant branch of the distribution, which is defined by the continuous mode and contains most of the BHs in our sample (see the contours), extends from $M_{\rm BH} \sim 10^2\,{\rm M}_\odot$ to $10^9\,{\rm M}_\odot$ and exhibits a positive correlation between $\dot{M}_{\rm BH}$ and $M_{\rm BH}$. The lower branch represents the passive population in which BH growth is halted either as the host galaxy becomes a satellite or the host halo temporarily makes an excursion to slow assembly. Of particular interest is the upper branch, which represents the population of nuclear bursts and is characterized by $\dot{M}_{\rm BH} \sim 10 \times \dot{M}_{\rm Edd}$, with the Eddington accretion rate defined as

$$\dot{M}_{\rm Edd} \equiv \frac{M_{\rm BH}}{\epsilon_{\rm r} t_{\rm Sal}} = 2.22 \times 10^{-2} \times \left(\frac{M_{\rm BH}}{10^6\,{\rm M}_\odot}\right)\left(\frac{\epsilon_{\rm r}}{0.1}\right)^{-1} {\rm M}_\odot{\rm yr}^{-1}\,. \quad (1)$$

Here, $t_{\rm Sal} = 0.450\,{\rm Gyr}$ is the Salpeter timescale, and $\epsilon_{\rm r} \sim 0.1$ is the radiative efficiency (e.g. F. Yuan & R. Narayan 2014; R. Weinberger et al. 2017).

Fig. 1b shows the distribution of BHs in the $f_{\rm BH}$-$M_{\rm BH}$ plane, where BH-mass fraction $f_{\rm BH} \equiv M_{\rm BH}/M_\star$ is defined as the ratio of BH mass to stellar mass of the host galaxy. The multi-channel growth of BHs can also be seen in this distribution. The frequent triggers of nuclear bursts in the early Universe can lead to a high BH-mass fraction of $f_{\rm BH} \approx 0.1$ – a consequence of the supernova-free nature of nuclear bursts and ineffective BH feedback due to photo-trapping at high accretion rate. The scatter of $f_{\rm BH}$ in this regime is large, due to the stochastic nature of the triggers and the rapid growth in individual bursts. In contrast, the continuous mode can sustain a lower $f_{\rm BH}$ with a smaller scatter due to the continuous capturing of sub-clouds and the regulation of BH growth by both stellar and BH feedback. The dominant channel of the BH growth makes a transition from the bursty mode to the continuous mode at $M_{\rm BH} \sim 10^6$–$10^7\,{\rm M}_\odot$, above which BHs are massive enough to generate strong feedback to effectively quench the bursty mode.

2.2. *Little red dots as black holes in super-Eddington accretion*

We use the following set of criteria to select LRDs from the predicted BH population at any given z.

1. The BH must accrete at a super-Eddington rate, $\dot{M}_{\rm BH} \geq \dot{M}_{\rm Edd}$. This criterion is motivated by theoretical considerations (e.g. A. de Graaff et al. 2025; D. Kido et al. 2025; R. P. Naidu et al. 2025a; H. Liu et al. 2025; K. Inayoshi et al. 2026; A. Trinca et al. 2026) that such an accretion is able to produce a gas envelope around the BH to explain the observed SED of LRDs. This selection also separates the LRD candidates from the dominant sub-Eddington branch in Fig. 1a, making the selected sample a distinct population rather than an extension of other BHs in the $\dot{M}_{\rm BH}$-$M_{\rm BH}$ plane.
2. The BH has a sufficiently high BHAR, $\dot{M}_{\rm BH} \geqslant \dot{M}_{\rm BH,min}$, so that it is luminous enough to be observed and identified as an LRD.
3. The BH-mass fraction is sufficiently high, $f_{\rm BH} \equiv M_{\rm BH}/M_\star \geq f_{\rm BH,min}$, so that the stellar component of the host galaxy is not too bright to obscure the spectral features of the BH.

The value of $\dot{M}_{\rm BH,min}$ depends on the detection limits of current observations. Here we take $\dot{M}_{\rm BH,min} = 0.1\,{\rm M}_\odot{\rm yr}^{-1}$ as the default to match the observed number density of LRDs at $z \gtrsim 4$ (see §3.1). We also use alternative criteria, with $\dot{M}_{\rm BH,min} = 0.05\,{\rm M}_\odot{\rm yr}^{-1}$ and $0.2\,{\rm M}_\odot{\rm yr}^{-1}$ to demonstrate the dependence on this threshold (see §3). These choices are also consistent with some other evaluations in the literature (e.g. M. C. Begelman & J. Dexter 2026; K. Inayoshi et al. 2026).

The other threshold, $f_{\rm BH,min}$, can be estimated using the condition that the total radiation from the BH dominates over that of the stellar component of the host galaxy so that AGN features are not overwhelmed by stellar lights. As suggested by the model implemented here (see Appendix C5 of Paper-IV), the bolometric luminosity ($L_{\rm BH}$) of a BH in super-Eddington accretion is limited to around the Eddington level,

$$L_{\rm BH} \approx L_{\rm Edd} = 3.28 \times 10^4\,{\rm L}_\odot \left(\frac{M_{\rm BH}}{{\rm M}_\odot}\right). \quad (2)$$

We estimate the bolometric luminosity of a stellar population younger than a few Myr using FSPS (C. Conroy et al. 2009; C. Conroy & J. E. Gunn 2010), as

$$L_\star \approx 10^3\,{\rm L}_\odot \left(\frac{M_\star}{{\rm M}_\odot}\right), \quad (3)$$

where a Chabrier IMF (G. Chabrier 2003) and a solar metallicity are assumed. The requirement of $L_{\rm BH} \geqslant L_\star$ then leads to a condition of $M_{\rm BH}/M_\star \geqslant 0.0304$. We thus set our default threshold of $f_{\rm BH,min} = 3\%$. We will discuss the effects of varying this threshold in §4.

Fig. 1 shows the boundaries of the default selection criterion (red solid lines) and regions enclosed by these boundaries (red shading) predicted at $z = 5$. BHs passing only the first two conditions are highlighted in blue, while those also passing the third one are highlighted in red. Alternative criteria with varied thresholds of $\dot{M}_{\rm BH}$ are also indicated (red dashed and dotted lines). The final sample at $z = 5$ based on the default criterion contains 41 LRDs in the simulation box, allowing a reliable analysis of the population. All modeled LRDs fall in the massive tip of the bursty branch in the $\dot{M}_{\rm BH}$-$M_{\rm BH}$ plane. *This pinpoints the bursty mode as the physical origin of LRDs, and indicates that the observed LRD population is the tip of an iceberg whose main body is hidden below the waterline set by the current detection limit.* This also explains why LRDs are not identified prior to JWST, as the tip level can only be reached with the JWST sensitivity. This is also consistent with the fact that no truncation is detected in the luminosity function of LRDs at the faint end (e.g. J. E. Greene et al. 2024; V. Kokorev et al. 2024; I. Labbe et al. 2025).

As shown in the following, our selection criterion is capable of reproducing key properties of the LRD population, such as the sharp drop of the number density at $z \lesssim 4$, the compact morphology, the blue UV part of the V-shape SED, and the stable UV-to-optical luminosity ratio, without fine-tuning the model. More importantly, our model treats the formation of LRDs within the same cosmological context as the formation of other populations of galaxies and BHs, and can make predictions that can be tested by observations.

3. MODEL PREDICTIONS

3.1. *The evolution of number density*

Fig. 2 shows the predicted number density (n) of LRDs as a function of z based on our default selection (solid red curve). For comparison, we show the observational results from Y. Ma et al. (2026) and V. Kokorev et al. (2024), and the empirical prediction by K. Inayoshi (2025). The number density of LRDs predicted by our model recovers the piece-wise evolution found in observations: a plateau at $z \gtrsim 4$ where the number density reaches a few times $10^{-5}\,{\rm cMpc}^{-3}$ and a sharp drop at $z \lesssim 4$.

The transition of BH growth and star formation from the bursty mode to the continuous mode (see §2.1 and Fig. 1b) provides a natural explanation for the observed drop of the number density of LRDs at $z \lesssim 4$. In the ΛCDM paradigm, halos with lower $M_{\rm halo}$ at lower z are expected to have slower assembly (F. Dong et al. 2022; W. Jiang et al. 2025), so that their excursions to nuclear bursts are rarer and star formation via the continuous

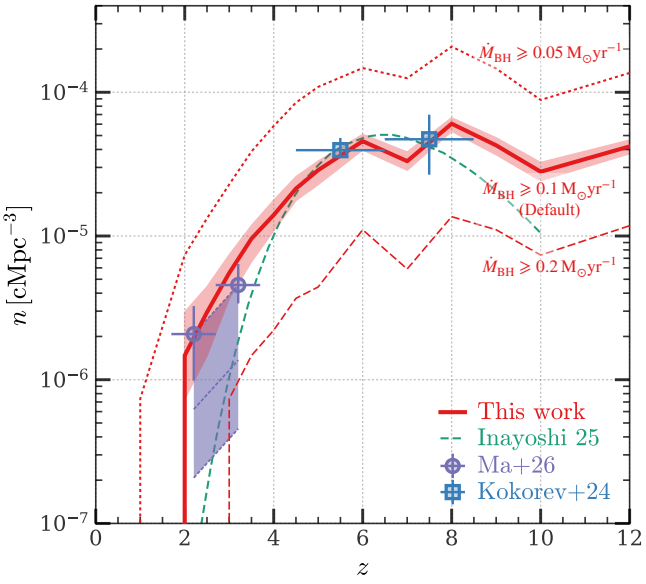

Figure 2. Number density of LRDs as a function of redshift. Here we show the predicted number density (n) of LRDs selected by our default criterion (**red solid**) and the criteria with alternative thresholds of $\dot{M}_{\rm BH}$ (**red dashed and dotted**). The curve with shading represents the median and $16^{\rm th}$–$84^{\rm th}$ percentile range of n among 100 random samples for the durations of nuclear bursts (see §2.1). For comparison, we show the observations by Y. Ma et al. (2026) and V. Kokorev et al. (2024), and empirical result of K. Inayoshi (2025). Three dotted lines associated with the **purple band** indicate the expected number density if 100%, 30% and 10%, respectively, of the selected candidates in Y. Ma et al. (2026) are LRDs. The model recovers the piece-wise evolution of LRD number density found in observations, and ties the physical origin of this evolution to the hierarchical nature of halo assembly that is determined by the ΛCDM cosmology (see §3.1 for details).

mode becomes more important. Consequently, halos that satisfy the three conditions for LRDs are increasingly rarer at lower z. *Our model thus ties the evolution of LRD number density to the halo assembly that is determined by the ΛCDM cosmology.*

Fig. 2 also shows the predicted number density of LRDs based on alternative selection criteria with $\dot{M}_{\rm BH}$ doubled or halved (red dashed and dotted curves). There is a factor of ~ 3 change in the predicted number density. This implies that ${\rm d}n\,/\,{\rm d}\dot{M}_{\rm BH} \propto \dot{M}_{\rm BH}^{-2.5}$ at $\dot{M}_{\rm BH} \sim 0.1\,{\rm M}_\odot{\rm yr}^{-1}$ for the BH growth driven by the bursty mode, and further supports the conclusion reached in §2.2 that a large population of LRDs is still hidden below the current detection limit.

3.2. *The progenitors and descendants of LRDs*

The complete coverage of our model from the seeding epoch to $z = 0$ allows us to predict the properties

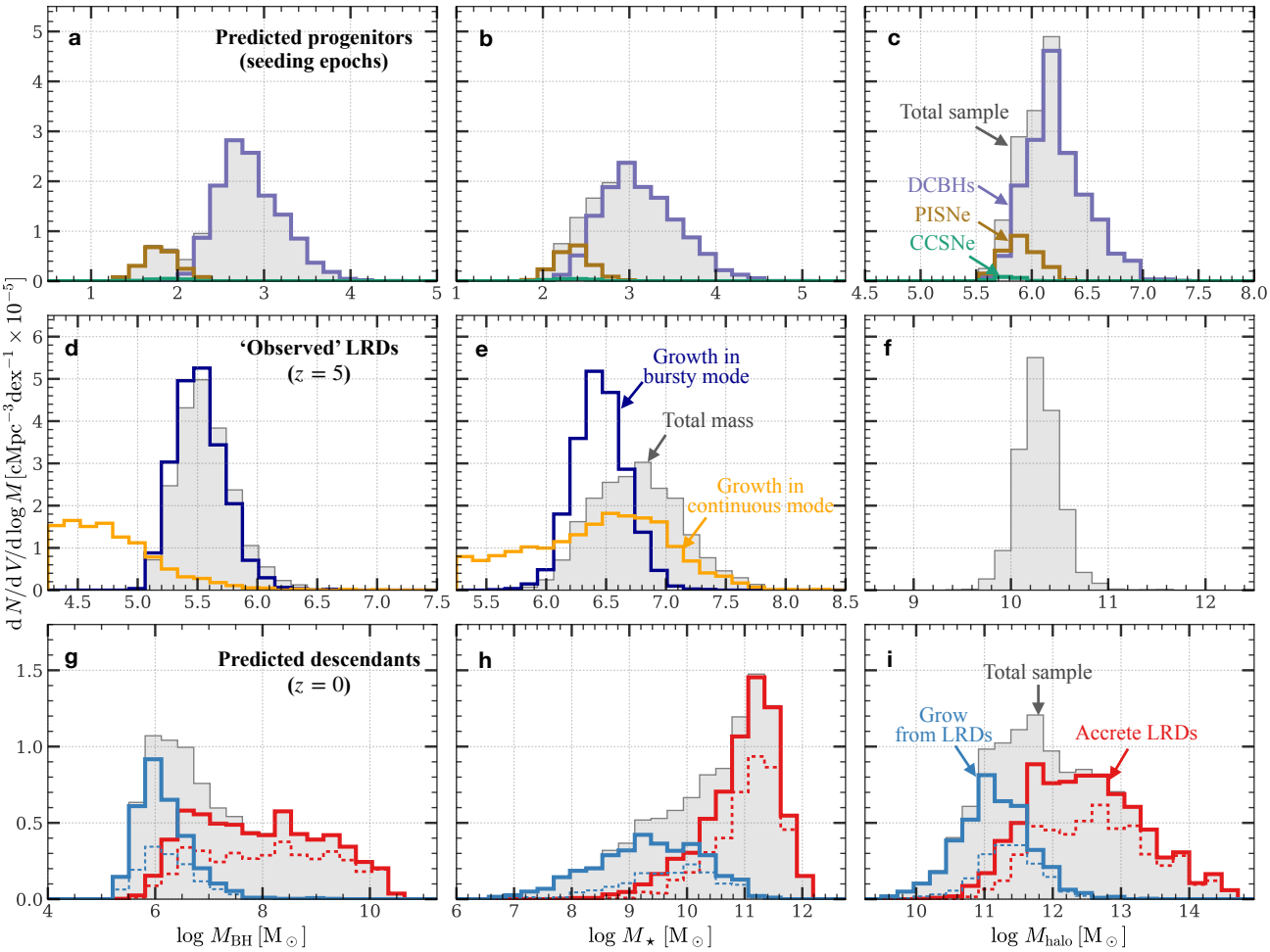

Figure 3. Distribution of properties of LRDs, their progenitors and descendants. The sample shown consists of LRDs at $z = 5$ with the default selection (see §2.2 and Fig. 1). 100 random samples for the durations of nuclear bursts (see §2.2) are drawn and averaged to suppress the sampling noise. The properties shown are $M_{\rm BH}$ of the BH, $M_\star$ of the host galaxy and $M_{\rm halo}$ of the host halo. For satellites, $M_{\rm halo}$ takes the infall value. The distributions are shown at three stages of their evolution: **a**–**c**, the seeding epochs (mostly $z \gtrsim 20$; identified backward in time through the main branch of merger tree); **d**–**f**, the "observed" epoch ($z = 5$); and **g**–**i**, the present day ($z = 0$; identified forward in time through descendant chain of merger tree). At seeding, sub-populations of seeds formed via DCBH, PISN, or CCSN are shown in total or separately. At $z = 5$, we show the distributions of the total mass and of those contributed by the bursty and continuous modes separately. At $z = 0$, we show the total sample of descendants, and sub-populations according to how an LRD is connected to its descendant: one includes descendants that grew from LRDs (i.e., LRDs lie on their main branches); the other includes descendants that accreted LRDs through mergers (i.e., LRDs lie on their side branches). Within each sub-population at $z = 0$, the subset of descendants that are central galaxies is also indicated (**dashed**). These archaeological and futurological views pinpoint the venues for the progenitors and descendants of LRDs to be found in observations (see §3.2 for details).

of LRDs, their progenitors at earlier epochs, and their descendants at later epochs, in a self-consistent cosmological context. Fig. 3 shows the predicted distributions of LRDs selected by the default criterion at three stages of evolution:

1. the seeding stage, at which the BH seeds of LRDs are formed as a result of the first collapse of gas in their host halos (see §2.1 for the seeding procedure);
2. the "observed" stage, taking $z = 5$ as the representative, at which BHs are selected as candidates of the observed LRD population;
3. the evolved stage, taking $z = 0$ as an example, at which LRDs have evolved into descendants to be observed in the local Universe.

At each stage, we show the distributions of $M_{\rm BH}$ of LRDs, $M_\star$ of their host galaxies, and $M_{\rm halo}$ of their host halos.

At seeding epochs, the BHs of LRD progenitors span a wide range of $M_{\rm BH}$, from $\sim 10\,{\rm M}_\odot$ to $\sim 10^4\,{\rm M}_\odot$ (Fig. 3a,

the gray histogram), indicating that diverse environmental processes (see §2.1) are operating to delay the gas cooling in the "mini-halos" and to elevate the mass of the first-generation stars formed in the collapsed gas. Although not shown here, the seeds of most LRDs are predicted to form at $z \gtrsim 20$. The early formation of these seeds, together with the predicted late occurrence of the IGM enrichment (see Fig. D4 of Paper-IV), implies that the seeds of LRDs are almost exclusively products of Pop-III stars. The top-heavy IMF assumed for Pop-III stars in the seeding procedure also implies that the initial $M_\star$ of the host galaxy is only a few times $M_{\rm BH}$ (Fig. 3b). Star formation efficiencies in the seeded mini-halos are as low as $M_\star/M_{\rm halo} \sim 10^{-3}$ (Fig. 3c), due to the dispersal of gas by the feedback from the first star cluster in the shallow potential well of such a mini-halo.

The stellar evolution implemented in the seeding procedure allows us to divide the seeds of LRDs into subpopulations of different flavors (formation pathways). The colored histograms in Fig. 3a show the distributions of seeds with CCSN, PISN and DCBH flavors, respectively. Most seeds are born as DCBHs from (super)massive progenitor stars with masses up to $\sim 10^4\,{\rm M}_\odot$. A significant fraction of seeds are born as remnants of secondary stars after the most massive one in the first cluster is destroyed by a PISN. This produces a significant mass gap and bimodality in the overall distribution of $M_{\rm BH}$. Only a small fraction of seeds are born as remnants of CCSN from low-mass progenitor stars, indicating that the origin of LRDs is quite different from that of stellar-mass BHs observed in the local Universe. The distribution of seed mass $M_{\rm BH}$ falls in the intermediate-mass BH (IMBHs) regime, which disfavors the interpretation that LRDs are powered by BHs formed directly from the first collapse in their host halos (e.g. J. F. W. Baggen et al. 2026). Instead, our model suggests that *it is post-seeding growth, mainly through episodic nuclear bursts, that raises BH seeds to supermassive status*. We note that the high masses of DCBH seeds are a prediction of our model, rather than a condition assumed to allow these BHs to reach the masses required to power LRDs.

At $z = 5$, the LRD population in our default selection have BHs with $M_{\rm BH} \sim 10^5$–$10^6\,{\rm M}_\odot$ (gray histogram in Fig. 3d). Decomposing the total $M_{\rm BH}$ into contributions from the bursty and continuous modes (colored histograms in Fig. 3d) reveals that the bursty mode dominates the BH growth. The $M_{\rm halo}$ of the host halos are about $\sim 10^{10}$–$10^{11}\,{\rm M}_\odot$ (Fig. 3f), comparable to those of dwarf galaxies in the local Universe (e.g. Z. Zhang et al. 2025). This predicted range of $M_{\rm halo}$ justifies our choice of simulation and halo sample to represent potential hosts of LRDs. The low $M_{\rm halo}$ implies a relatively weak clustering of LRDs in space, a conclusion that is consistent with recent observations (M. Carranza-Escudero et al. 2025).

The $M_\star$ of LRDs is predicted to be $\sim 10^6$–$10^{7.5}\,{\rm M}_\odot$ (Fig. 3e), roughly an order of magnitude higher than $M_{\rm BH}$, consistent with the high BH-mass fraction, $f_{\rm BH} \sim 0.1$, expected from the growth driven by the bursty mode (see Fig. 1b). Indeed, decomposing the total $M_\star$ into contributions from the bursty and continuous modes (colored histograms in Fig. 3e) shows that the bursty mode contributes significantly to the total $M_\star$ of LRDs, while the contribution of the continuous mode is only marginally higher than that of the bursty mode. Our model thus suggests that LRDs are transitional objects in which the continuous mode of star formation is about to take over the burst mode, and that the extended stellar components are about to be built up in the host galaxies. The dominance of nuclear bursts in the growth of LRDs may thus provide an explanation for their observed compact morphology.

Young stellar populations formed via nuclear bursts in an LRD are expected to produce a blue UV component in the SED (J. E. Greene et al. 2024; I. Labbe et al. 2025, e.g.). This, together with the red optical component produced by the BH in super-Eddington accretion, offers a compelling explanation for the observed V-shape SED of LRDs. In addition, the stable $f_{\rm BH} \sim 0.1$ produced by the bursty mode (see Fig. 1b) implies a near-constant optical-to-UV luminosity ratio ($L_{\rm opt}/L_{\rm UV}$). Such a constant luminosity ratio is found in recent observations, and the value of $f_{\rm BH} \sim 0.1$ predicted by our model also aligns with those inferred from the SEDs of LRDs (e.g. K. Inayoshi et al. 2026).

The descendants of LRDs at $z = 0$ show a broad distribution of $M_{\rm BH}$ (Fig. 3g), reflecting the diverse evolutionary pathways of LRDs after the observed epoch. Some LRDs merge into massive galaxies covering a wide range in $M_{\rm BH}$, $M_\star$, and $M_{\rm halo}$, from dwarf galaxies to the brightest cluster galaxies (BCGs) in massive clusters (red solid in Fig. 3g–i). Other LRDs evolve along more isolated pathways, growing as the main progenitors of their descendants and dominating the lower ends of the mass distributions (blue solid in Fig. 3g–i). The typical $M_{\rm BH}$ of these low-mass descendants is $\sim 10^6\,{\rm M}_\odot$, only a factor of three higher than the typical $M_{\rm BH}$ of LRDs at $z = 5$, implying that their BHs have experienced little growth since $z = 5$ and their NSCs are predicted to contain a significant fraction of ancient stars formed via nuclear bursts at high z. However, the total $M_\star$ of these low-mass descendants is ~ 2–$3\,{\rm dex}$ higher than that of the LRDs at $z = 5$, implying that extended stellar components have been built up in the descendants. About half of the low-mass descendants remain isolated (blue dashed in Fig. 3g–i); the other half are satellites, susceptible to tidal forces that may strip their extended stellar masses. This implies a diverse, environment-driven morphology for the descendants, ranging from nucleated dwarfs with extended stellar components, if they remain isolated, to compact objects such as ultra-compact dwarfs (UCDs) or globular-like star clusters, if most of the extended stellar masses have been stripped away.

We note that the predicted properties and evolution of LRDs depend on the selection criterion, which itself varies between observational studies. In addition to the dependence of the number density on the luminosity threshold controlled by $\dot{M}_{\rm BH,min}$ (see §3.1 and Fig. 2), the threshold $f_{\rm BH,min}$ also has a noticeable impact on the prediction. For example, removing the $f_{\rm BH}$ threshold leads to a larger number of LRDs, higher $M_{\rm BH}$ and $M_\star$, and a higher fraction of $M_\star$ in their extended stellar components. The $M_{\rm BH}$ of LRDs may thus reach $\sim 10^7\,{\rm M}_\odot$ if those having larger stellar components are included in the sample (e.g. blue points in Fig. 1). Despite such uncertainties in sample selections, our predictions are broadly consistent with observations: the predicted $M_{\rm BH}\approx 10^5$–$10^7\,{\rm M}_\odot$ for LRDs aligns with those reported by J. E. Greene et al. (2026); the existence of young, extended stellar components in the host galaxies aligns with recent stacking analysis that reveals extended, wavelength-dependent emission around LRDs (Y. Zhang et al. 2025); the co-existence of NSCs and extended stellar components suggests a bimodal origin of the rest-frame UV emission, which may explain the observed dichotomy in the distribution of UV half-light radii of LRDs (A. P. Cloonan et al. 2026).

4. SUMMARY AND DISCUSSION

In this paper, we have applied the model of galaxy formation developed in Paper-IV to study the physical origin of LRDs, to interpret their observed properties, and to make predictions for their progenitors and descendants over the cosmic time.

Our key finding is that LRDs emerge as a "tip-of-iceberg" population of BHs in super-Eddington accretion, associated with the ongoing formation of compact NSCs and with extended stellar components that are about to be built in their host galaxies (§2; Fig. 1). The emergence of this population is driven by nuclear bursts triggered by global disturbances, such as mergers or close encounters, which can remove the angular-momentum barrier, funnel gas inward to form a gas-rich, compact, supernova-free nucleus, and sustain the super-Eddington BH growth and nuclear star formation over a short timescale of $\lesssim$ Myr. The origin of such global disturbances is tied to excursions to a fast phase in the assembly histories of host halos, suggesting that the LRD population may be a natural consequence of hierarchical structure formation in the ΛCDM cosmology.

Our model is among the first to self-consistently include the formation of seeds and the BH-galaxy-halo co-evolution within a cosmological context, allowing the emergence of the LRD population as a natural outcome of the ΛCDM paradigm, rather than a result of fine-tuning. In fact, none of the model prescriptions or parameters was designed or tuned according to the observations of the LRDs. The strength of the halo excursion required to trigger a nuclear burst is set to the same value that separates the two phases of ΛCDM halos (see Eq. C3 of Paper-IV and §2 of Paper-I); the efficiency of star formation in nuclear star bursts is set by the free-fall timescale and the BH accretion there is modeled on-the-fly using a turbulence-modified Bondi accretion plus a turbulent and magnetized accretion disk (see Appendix C of Paper-IV); the mass loading of AGN feedback in nuclear bursts is determined by the Eddington-level luminosity and a typical outflow velocity of $10^3\,{\rm km\,s^{-1}}$ (see Appendix C5 of Paper-IV).

The LRD population predicted by our model reproduces a broad range of observations, and our model can make predictions for many more properties of the LRD population themselves, as well as their progenitors and descendants (§3; Figs. 2 and 3). This allows the prescriptions implemented in the model to be tested by observations targeting different evolution stages of LRDs and the differences from other models to be explicitly examined. We discuss some of these aspects below.

Although the BH* scenario has previously been suggested and accepted as a promising interpretation of LRDs, our model provides a physical framework to explain how the conditions required for BH* formation are created in the galaxy formation context. Our model differs from other models that interpret LRDs as (DC)BHs formed in the first collapses of the halo gas (J. F. W. Baggen et al. 2026). For example, the LRDs at $z=5$ predicted by our model are seeded at $z\gtrsim 20$ and have since gone through ~ 10 episodes of nuclear bursts (see Fig. 9 of Paper-IV) interspersed with phases of continuous growth. Our model differs from that suggested by K. Inayoshi et al. (2026) in the following aspects: the shining phase of an LRD in our model is a violent and bursty event, episodically triggered by global disturbance, asynchronous with the evolution of their host galaxies, and lasting for $\lesssim 1\,{\rm Myr}$, instead of a secular process over $\gtrsim 10\,{\rm Myr}$ in the nuclear region extrapolated from the host galactic disk; the observed LRDs in our model are objects with significant post-seeding growth, instead of nascent BHs embedded in nascent star-forming galaxies; the depletion of gas in nuclear regions is mostly driven by the feedback from the accreting BHs, rather than stellar feedback.

A unique consequence of episodic bursts in our model is that the LRDs currently observed are just the tip of the iceberg shaped by bursty-mode growth (see Fig. 1a). Observations with improved sensitivity are thus expected to reveal many more BHs below the waterline of the current detection limit. Another consequence is that the companion NSC of an LRD should harbor a significant fraction of ancient stars formed through previous nuclear bursts since $z\gtrsim 20$ and, at the same time, possess a large fraction of young stars with age $\lesssim 1\,{\rm Myr}$ formed during the ongoing burst. This prediction may be tested by observations that can resolve individual stellar populations through SED or spatial decompositions. The "about-to-be-built" extended stellar components in the host galaxies of LRDs also suggest that some observed

LRDs may already have built up extended stellar components that can be revealed by stacking analysis and by deep imaging observations (e.g. Y. Zhang et al. 2025; A. P. Cloonan et al. 2026).

The complete coverage of the evolution history of the LRD population by our model allows us to seek observational evidence for both the seeding and growing processes through archaeology of their descendants at lower z. For example, the mass gap of the BH-seed mass function produced by PISNe may lead to a bimodal distribution of galaxies in their post-seeding star formation, provided that the effects of BH feedback depend on BH mass. Observations targeting galaxies at $z \gtrsim 10$ (e.g. R. Maiolino et al. 2024; S. Tacchella et al. 2023; X. Ji et al. 2025b; Á. Bogdán et al. 2023; R. P. Naidu et al. 2025b; S. Carniani et al. 2024; E. Curtis-Lake et al. 2023), before the evolution of BHs and their host galaxies converges due to self-regulation (see §3.3.2 and Fig. 11 of Paper-IV), may be able to identify such a bimodality. Another implication of the model is that LRDs seeded after PISNe should be associated with stars enriched by the ejecta of PISNe. The peculiar abundance patterns of PISN enrichment, as seen in a small set of stars discovered in the local Universe (e.g. Q.-F. Xing et al. 2023; Á. Skúladóttir et al. 2024), may thus be used to link the descendants of LRDs to their seeding pathways.

As shown by the blue histogram in Fig. 3g–i, our model predicts that a significant fraction of the LRD population gained only modest amounts in mass and the stellar mass of the descendants matches that of dwarf galaxies in the local Universe. These descendants are predicted to harbor BHs with $M_{\rm BH}$ similar to those of LRDs and to have a significant fraction of $M_\star$ formed during the early bursty growth. In particular, the absence of large amounts of growth suggests that such a descendant should contain a compact component formed through early nuclear bursts, reminiscent of an ultra-compact dwarf (UCD) or the central part of a nucleated dwarf (e.g. K. Wang et al. 2023). We will present a detailed analysis of the connection between LRDs and present-day compact dwarf galaxies in a forthcoming paper.

ACKNOWLEDGMENTS

This work is supported by Double First-Class Discipline Construction-Astronomy Discipline at Nanjing University, the National Natural Science Foundation of China (Grant no. 12503014), and the Fundamental Research Funds for the Central Universities (Grant no. KG202502). The authors thank Tao Wang, Enci Wang and Zhaozhou Li for their discussions and insights, and thank Yi Mao and Chen Chen for their technical support. The authors would like to express their gratitude to the Tsinghua Astrophysics High-Performance Computing platform at Tsinghua University for providing the necessary computational and data storage resources that have significantly contributed to the research results presented in this paper.

AUTHOR CONTRIBUTIONS

The authors contributed equally to this work.

Software: Hipp (Y. Chen & K. Wang 2023), Astropy (T. P. Robitaille et al. 2013; Astropy Collaboration et al. 2018, 2022), SatGen(F. Jiang et al. 2021), WebPlotDigitizer .

Data availability: Codes implementing our model, catalogs produced by the model, and data and scripts to reproduce all figures will be available at the repository TwoPhaseGalaxyModel (https://github.com/ChenYangyao/two-phase-galaxy-model). The N-body data have been made public by the IllustrisTNG project (https://www.tng-project.org/).

REFERENCES

Akins, H. B., Casey, C. M., Lambrides, E., et al. 2025, ApJ, 991, 37, doi: 10.3847/1538-4357/ade984

Asada, Y., Sawicki, M., Abraham, R., et al. 2024, MNRAS, 527, 11372, doi: 10.1093/mnras/stad3902

Astropy Collaboration, Price-Whelan, A. M., Sipőcz, B. M., et al. 2018, AJ, 156, 123, doi: 10.3847/1538-3881/aabc4f

Astropy Collaboration, Price-Whelan, A. M., Lim, P. L., et al. 2022, ApJ, 935, 167, doi: 10.3847/1538-4357/ac7c74

Baggen, J. F. W., Scoggins, M. T., van Dokkum, P., et al. 2026, ApJ, 1002, L4, doi: 10.3847/2041-8213/ae58a5

Begelman, M. C., & Dexter, J. 2026, ApJ, 996, 48, doi: 10.3847/1538-4357/ae274a

Bogdán, Á., Goulding, A. D., Natarajan, P., et al. 2023, Nature Astronomy, 8, 126, doi: 10.1038/s41550-023-02111-9

Carniani, S., Hainline, K., D'Eugenio, F., et al. 2024, Nature, 633, 318, doi: 10.1038/s41586-024-07860-9

Carranza-Escudero, M., Conselice, C. J., Adams, N., et al. 2025, ApJ, 989, L50, doi: 10.3847/2041-8213/adf73d

Chabrier, G. 2003, Publications of the Astronomical Society of the Pacific, 115, 763, doi: 10.1086/376392

Chen, C.-H., Ho, L. C., Li, R., & Zhuang, M.-Y. 2025, ApJ, 983, 60, doi: 10.3847/1538-4357/ada93a

Chen, Y., Mo, H., & Wang, H. 2024, MNRAS, 532, 4340, doi: 10.1093/mnras/stae1757

Chen, Y., Mo, H., & Wang, H. 2025a, A Two-Phase Model of Galaxy Formation: IV. Seeding and Growing Supermassive Black Holes in Dark Matter Halos, arXiv, doi: 10.48550/arXiv.2509.03283

Chen, Y., Mo, H., & Wang, H. 2025b, MNRAS, 540, 1235, doi: 10.1093/mnras/staf791

Chen, Y., & Wang, K. 2023, Astrophysics Source Code Library, ascl:2301.030. https://ui.adsabs.harvard.edu/abs/2023ascl.soft01030C

Cloonan, A. P., Whitaker, K. E., Manning, S. M., et al. 2026, arXiv e-prints, arXiv:2603.24700, doi: 10.48550/arXiv.2603.24700

Conroy, C., & Gunn, J. E. 2010, ApJ, 712, 833, doi: 10.1088/0004-637X/712/2/833

Conroy, C., Gunn, J. E., & White, M. 2009, ApJ, 699, 486, doi: 10.1088/0004-637X/699/1/486

Crain, R. A., Schaye, J., Bower, R. G., et al. 2015, MNRAS, 450, 1937, doi: 10.1093/mnras/stv725

Curtis-Lake, E., Carniani, S., Cameron, A., et al. 2023, Nature Astronomy, 7, 622, doi: 10.1038/s41550-023-01918-w

de Graaff, A., Rix, H.-W., Naidu, R. P., et al. 2025, A&A, 701, A168, doi: 10.1051/0004-6361/202554681

Dong, F., Zhao, D., Han, J., et al. 2022, ApJ, 929, 120, doi: 10.3847/1538-4357/ac5aaa

El-Badry, K., Wetzel, A., Geha, M., et al. 2016, ApJ, 820, 131, doi: 10.3847/0004-637X/820/2/131

Greene, J. E., Labbe, I., Goulding, A. D., et al. 2024, ApJ, 964, 39, doi: 10.3847/1538-4357/ad1e5f

Greene, J. E., Setton, D. J., Furtak, L. J., et al. 2026, ApJ, 996, 129, doi: 10.3847/1538-4357/ae1836

Greif, T. H., White, S. D. M., Klessen, R. S., & Springel, V. 2011, ApJ, 736, 147, doi: 10.1088/0004-637X/736/2/147

Hopkins, P. F., Gurvich, A. B., Shen, X., et al. 2023, MNRAS, 525, 2241, doi: 10.1093/mnras/stad1902

Hopkins, P. F., Grudic, M. Y., Su, K.-Y., et al. 2024, The Open Journal of Astrophysics, 7, 18, doi: 10.21105/astro.2309.13115

Inayoshi, K. 2025, ApJL, 988, L22, doi: 10.3847/2041-8213/adea66

Inayoshi, K., Murase, K., & Kashiyama, K. 2026, ApJ, 1000, 90, doi: 10.3847/1538-4357/ae42ce

Ji, X., Maiolino, R., Übler, H., et al. 2025a, BlackTHUNDER – A Non-Stellar Balmer Break in a Black Hole-Dominated Little Red Dot at $z=7.04$, arXiv, doi: 10.48550/arXiv.2501.13082

Ji, X., Maiolino, R., Ferland, G., et al. 2025b, MNRAS, 541, 2134, doi: 10.1093/mnras/staf1083

Jiang, F., Dekel, A., Freundlich, J., et al. 2021, MNRAS, 502, 621, doi: 10.1093/mnras/staa4034

Jiang, F., Jia, Z., Zheng, H., et al. 2025, Formation of the Little Red Dots from the Core-collapse of Self-interacting Dark Matter Halos, arXiv, doi: 10.48550/arXiv.2503.23710

Jiang, W., Han, J., Dong, F., & He, F. 2025, ApJ, 988, 160, doi: 10.3847/1538-4357/ade439

Kido, D., Ioka, K., Hotokezaka, K., Inayoshi, K., & Irwin, C. M. 2025, MNRAS, 544, 3407, doi: 10.1093/mnras/staf1898

Kokorev, V., Caputi, K. I., Greene, J. E., et al. 2024, ApJ, 968, 38, doi: 10.3847/1538-4357/ad4265

Koudmani, S., Somerville, R. S., Sijacki, D., et al. 2024, MNRAS, 532, 60, doi: 10.1093/mnras/stae1422

Labbe, I., Greene, J. E., Bezanson, R., et al. 2025, ApJ, 978, 92, doi: 10.3847/1538-4357/ad3551

Latif, M. A., Whalen, D. J., Khochfar, S., Herrington, N. P., & Woods, T. E. 2022, Nature, 607, 48, doi: 10.1038/s41586-022-04813-y

Li, H., Chen, Y., Wang, H., & Mo, H. 2025, MNRAS, 543, 1878, doi: 10.1093/mnras/staf1594

Li, Z., Inayoshi, K., Chen, K., Ichikawa, K., & Ho, L. C. 2025, ApJ, 980, 36, doi: 10.3847/1538-4357/ada5fb

Liu, H., Jiang, Y.-F., Quataert, E., Greene, J. E., & Ma, Y. 2025, ApJ, 994, 113, doi: 10.3847/1538-4357/ae0c19

Ma, Q., Chen, Y., & Mo, H. 2026, MNRAS, 548, stag562, doi: 10.1093/mnras/stag562

Ma, Y., Greene, J. E., Setton, D. J., et al. 2026, ApJ, 1000, 59, doi: 10.3847/1538-4357/ae4596

Maiolino, R., Scholtz, J., Witstok, J., et al. 2024, Nature, 627, 59, doi: 10.1038/s41586-024-07052-5

Matthee, J., Naidu, R. P., Brammer, G., et al. 2024, ApJ, 963, 129, doi: 10.3847/1538-4357/ad2345

Mo, H., Chen, Y., & Wang, H. 2024, MNRAS, 532, 3808, doi: 10.1093/mnras/stae1727

Naidu, R. P., Matthee, J., Katz, H., et al. 2025a, A "Black Hole Star" Reveals the Remarkable Gas-Enshrouded Hearts of the Little Red Dots, arXiv, doi: 10.48550/arXiv.2503.16596

Naidu, R. P., Oesch, P. A., Brammer, G., et al. 2025b, A Cosmic Miracle: A Remarkably Luminous Galaxy at $z_{\rm{spec}}=14.44$ Confirmed with JWST, arXiv, doi: 10.48550/arXiv.2505.11263

Nelson, D., Springel, V., Pillepich, A., et al. 2019, Computational Astrophysics and Cosmology, 6, 2, doi: 10.1186/s40668-019-0028-x

Pérez-González, P. G., Barro, G., Rieke, G. H., et al. 2024, ApJ, 968, 4, doi: 10.3847/1538-4357/ad38bb

Perger, K., Fogasy, J., Frey, S., & Gabányi, K. É. 2025, A&A, 693, L2, doi: 10.1051/0004-6361/202452422

Pillepich, A., Nelson, D., Hernquist, L., et al. 2018, MNRAS, 475, 648, doi: 10.1093/mnras/stx3112

Planck Collaboration, Ade, P. A. R., Aghanim, N., et al. 2016, A&A, 594, A13, doi: 10.1051/0004-6361/201525830

Roberts, M. G., Braff, L., Garg, A., Profumo, S., & Jeltema, T. 2026, Journal of Cosmology and Astroparticle Physics, 2026, 003, doi: 10.1088/1475-7516/2026/05/003

Robitaille, T. P., Tollerud, E. J., Greenfield, P., et al. 2013, A&A, 558, A33, doi: 10.1051/0004-6361/201322068

Sijacki, D., Springel, V., Di Matteo, T., & Hernquist, L. 2007, MNRAS, 380, 877, doi: 10.1111/j.1365-2966.2007.12153.x

Sivasankaran, A., Blecha, L., Torrey, P., et al. 2025, MNRAS, 537, 817, doi: 10.1093/mnras/staf062

Skúladóttir, Á., Koutsouridou, I., Vanni, I., et al. 2024, ApJ, 968, L23, doi: 10.3847/2041-8213/ad4b1a

Somerville, R. S., Hopkins, P. F., Cox, T. J., Robertson, B. E., & Hernquist, L. 2008, MNRAS, 391, 481, doi: 10.1111/j.1365-2966.2008.13805.x

Spinoso, D., Bonoli, S., Valiante, R., Schneider, R., & Izquierdo-Villalba, D. 2023, MNRAS, 518, 4672, doi: 10.1093/mnras/stac3169

Stern, J., Faucher-Giguère, C.-A., Fielding, D., et al. 2021, ApJ, 911, 88, doi: 10.3847/1538-4357/abd776

Su, K.-Y., Bryan, G. L., Haiman, Z., et al. 2023, MNRAS, 520, 4258, doi: 10.1093/mnras/stad252

Tacchella, S., Eisenstein, D. J., Hainline, K., et al. 2023, ApJ, 952, 74, doi: 10.3847/1538-4357/acdbc6

Trinca, A., Lupi, A., Haardt, F., & Madau, P. 2026, You Can't See Me: Super-Eddington Growth Hindering X-ray Detection in High-z Broad-Line AGNs, arXiv, doi: 10.48550/arXiv.2602.22305

Wang, K., Peng, E. W., Liu, C., et al. 2023, Nature, 623, 296, doi: 10.1038/s41586-023-06650-z

Wang, Z., Jiang, F., Zheng, H., et al. 2026, Halo Assembly Bias in the Early Universe: A Clustering Probe of the Origin of the Little Red Dots, arXiv, doi: 10.48550/arXiv.2603.15736

Weinberger, R., Springel, V., Hernquist, L., et al. 2017, MNRAS, 465, 3291, doi: 10.1093/mnras/stw2944

Wise, J. H., Regan, J. A., O'Shea, B. W., et al. 2019, Nature, 566, 85, doi: 10.1038/s41586-019-0873-4

Xing, Q.-F., Zhao, G., Liu, Z.-W., et al. 2023, Nature, 618, 712, doi: 10.1038/s41586-023-06028-1

Yuan, F., & Narayan, R. 2014, ARA&A, 52, 529, doi: 10.1146/annurev-astro-082812-141003

Yue, M., Eilers, A.-C., Ananna, T. T., et al. 2024, ApJ, 974, L26, doi: 10.3847/2041-8213/ad7eba

Zhang, Y., Ding, X., Yang, L., et al. 2025, Unveiling Extended Components of 'Little Red Dots' in Rest-Frame Optical, arXiv, doi: 10.48550/arXiv.2510.25830

Zhang, Z., Chen, Y., Rong, Y., et al. 2025, Nature, 642, 47, doi: 10.1038/s41586-025-08965-5